Comparative Study of the Electromagnetic Performance of Yokeless and Segmented Armature YASA Machine with Different Rotor Pole Combinations

Mohammed F. KHATAB
Department of Electrical & Electronic Engineering
Mohammed.khtab@omu.edu.ly

Aiman NOUH
Department of Electrical & Electronic Engineering
aiman.nouh@omu.edu.ly

Department of Electrical and Electronics Engineering, College of Engineering University of Omar Al-Mukhtar - Al-Bayda, Libya

ABSTRACT

In this paper, a conventional axial flux yokeless and segmented armature YASA machine is designed and then simulated. It has been proved that, this machine has a high torque density and has been utilized for wind generation and electric vehicle applications. With 12 stator segments, different rotor pole combinations are designed. To maximize the machine torque, the topology is optimized by means of three-dimensional finite element analysis (3D-FEA). The electromagnetic performance for different pole combinations is then analysed and compared. It has been found that the machine with 16 and 14 rotor poles both have high torques. However, the machine with 14 rotor pole has better torque quality and back EMF compared with the other rotor pole combinations

Keywords: PM machines, axial flux machines, YASA machine, electromagnetic performance .

1 Introduction

With the aim of improving the winding arrangements and eliminating the yoke iron so as to reduce the iron loss in the axial flux TORUS machine, a Yokeless and Segmented Armature (YASA) axial field permanent magnet machine was initially developed and prototyped for automotive applications in [1]. The machine was formed by removing the stator yoke of the TORUS type since the flux of this topology passes axially through the stator poles. Compared to other axial flux machines, the YASA machine has the merits of short end windings, high efficiency, high torque density, high winding packing factor and easily fitted stator poles[2] [3]. However, since the stator is a combination of iron pieces, the mechanical design of the stator pole holder is still vitally important due to the axial force exerted between the stator and the rotors. This is the main drawback of double rotor axial flux machines [4].

Numerous studies have been devoted to the YASA machine performance analysis and manufacturing fabrication for different applications, for example wind generation and electric vehicles. It was first presented and prototyped for a sports vehicle in [1] and [2]. With torque density of 17.6 Nm/Kg, a 10-pole, 12-stator segment prototype was developed, and Soft magnetic composite (SMC) material used for the machine stator segments. For in–wheel direct drive traction applications, 10 poles and 12 stator

segments, a 6 kW YASA machine was investigated in [5]. In [3], a 16-pole and a 15-stator segment YASA generator was designed and prototyped. The experimental results show that an efficiency of approximately 87% was obtained at rated speed. In [6], YASA machines were compared to the conventional Radial flux PM (RFPM) and Axial flux PM (AFPM) machines. The comparative investigation found that the YASA machine has a significantly higher torque density as well as low active material weight.

It has been found that internal stator AFPM machine topologies have been extensively developed and investigated for drive applications. Moreover, a YASA machine has superior performance amongst internal stator AFPM topologies. Furthermore, it has been found that based on a performance comparison of AFPM machine topologies, a YASA machine is inherently suited to direct drive application [2] [7]. Therefore, in this paper, since this machine has a unique topology, the machine performance will be investigated in order to provide a baseline of comparison for the subsequent proposed axial field machines. With 12 stator segments, the machine is designed and optimized with different rotor pole combinations. A performance comparison between YASA machine topologies at no-load and on-load conditions will be investigated. Moreover, the torque performance with respect to the current, current density and copper loss will be obtained and compared.

2 YASA Machine Configuration and Principle Of Operation

A YASA machine, as illustrated in Figure 1, has double rotors with PMs mounted on two opposing rotor discs, and a single stator between both PM rotors. The stator is individually segmented and stacked together with high strength material holder to form magnetically isolated stator poles. Moreover, fractional slot concentrated windings are wound around each of the individual stator poles and connected to form the stator phase windings.

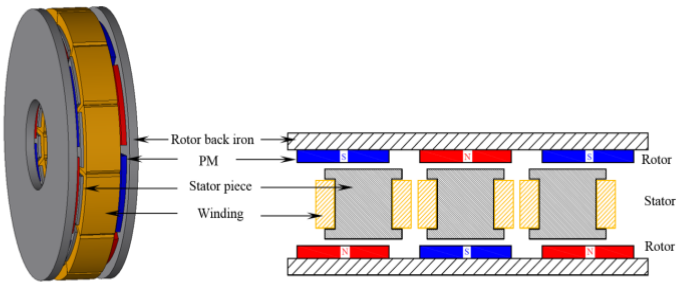

Figure 1 . *YASA machine configuration.*

For a given volume of PM machines and for a specific of phase number, the design is essentially based on obtaining a combination of the stator and rotor pole pairs. The phase number is selected as three in this study, and therefore, for double layer 3-phase windings of YASA machine, the number of stator segments must be a multiple of 3 and the phases are shifted by 120 elec. deg. Moreover, for balanced magnetic pall as well as high winding factor, the PM machine stator and rotor pole numbers should be related by [8] [9]:

$$n_s = 2p \pm 2 \quad (1)$$

A 12 poles with concentrated windings has been chosen for the YASA machine stator. The coils are connected in series to form the stator phase windings. The selection of appropriate combination of slot and pole numbers should ensure the winding distribution balance in the machines. The number of slots per pole per phase (S_p) can be calculated by [10]:

$$S_{pp} = \frac{n_s}{2pm} \quad (2)$$

where m is the number of phases.

Consequently, the most appropriate stator and rotor pole combination can be obtained by (1), when k is even. Table 1 lists the possible rotor pole combinations, their S_{pp} and the fundamental winding factor k_{w1} for n_s of 12 poles. The fundamental winding factor for double-layer concentrated windings is calculated by[11]:

$$K_{w1} = K_{d1}\, K_{p1} \quad (3)$$

where K_{d1} and K_{p1} are the main harmonic distribution and pitch factors, respectively.

It has been confirmed that high winding factor and balanced concentrated windings are normally adopted when $0.25 \leq S_{pp} \leq 0.5$ [10]. The winding distribution whereby $S_{pp} < 0.25$ has a low fundamental winding factor causing a non-sinusoidal back EMF (i.e. 12/20, 12/22). Moreover, the pole combinations which have $S_{pp} > 0.5$, (i.e. 12/2, 12/4) and where S_{pp} is thus an integer must have distributed winding to obtain a high winding factor. In terms of the rotor pole combinations listed in **Table *1***, for YASA machine and due to the focus of this study, this paper only explores YASA with $0.25 \leq S_{pp} \leq 0.5$ in which a high winding factor is gained.

Table 1*: Rotor pole combinations for 12-slots, 3-phase concentrated windings*

Name	2p	S_{pp}	K_{d1}	K_{p1}	K_{w1}
YASA12/22	22	0.18	0.966	0.25	0.25
YASA12/20	20	0.2	1	0.5	0.5
YASA12/16	16	0.25	1	0.866	0.866
YASA12/14	14	0.28	0.966	0.966	0.933
YASA12/10	10	0.4	0.966	0.966	0.933
YASA12/8	8	0.5	1	0.866	0.866
YASA12/4	4	1	1	0.5	0.5
YASA12/2	2	2	0.966	0.25	0.25

For the selected rotor pole combinations, the distributions of the phase coils are determined by the induced back EMF phasor in each coil. The coils distributions for the proposed pole combination are illustrated in Figure 2. Moreover, since the machine has 12 stator poles connected as a three-phase

machine, each phase comprises four coils. Furthermore, for the topologies with 0.5> S_{pp} >0.25 (i.e.YASA12/10, YASA12/14), two successive stator segments are wound with coils of the same phase. In this case, a high fundamental winding factor can be obtained. However, the topologies with S_{pp}= 0.5 and 0.25, (i.e. YASA12/8, YASA12/16) have a relatively low fundamental winding factor of 0.866.

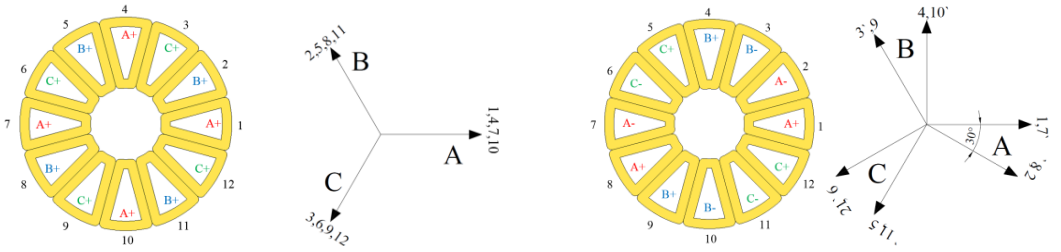

(a) YASA12/8 and YASA12/16 *(b) YASA12/10 and YASA12/14*

Figure 2 : *Coils arrangments and the EMF phasor for YASA machines with different slot/pole number combinations.*

3 Comparison Of Machine Performance For Different Rotor Pole Combinations

With the aim of comparing rotor pole combinations of YASA machine, the optimized machines were designed and analysed with the aid of JMAG 3-D FEA software. The optimal dimensions and the machine parameters are compared and listed in Table 2. The machine topologies were studied at no-load and on-load conditions, details of which can be found in the following sections.

3.1 Cogging Torque

Cogging torque exists in PM machines because of the variation of the permeance of air-gap due to stator slots. Therefore, the interaction of the permeance harmonics and the magnet MMF harmonics results in unwanted torque harmonics and thus torque pulsating.

The cogging torque was studied for the selected YASA machine topologies. Figure 3 compares the cogging torques and the corresponding harmonics for YASA machine topologies. YASA12/8 has the highest peak-peak cogging torque while YASA12/10 has the lowest cogging torque. The cogging torque level can be estimated for the slot and pole number combinations of PM machines by the cogging torque factor C_T which can be expressed as indicated in [14] as:

$$C_T = \frac{2p\ n_s}{N_C} \qquad (4)$$

where: N_C is the least common multiple between the number of stator poles and the number of rotor pole.

Higher C_T value indicates higher cogging torque value. However, the minimum value for C_T is unity, which constitutes a proper selection for rotor pole pair combination. For YASA12/8 and YASA12/16, the cogging torque factor is 4. It equals 2 for YASA12/10 and YASA12/14.

Table 2*: YASA machine pole combination optimal dimensions and parameters*

Parameter	YASA 12/8	YASA 12/10	YASA 12/14	YASA 12/16
Rated speed (RPM)	400	400	400	400
Rotor pole no. ($2p$)	8	10	14	16
Stator slot no. (n_s)	12	12	12	12
Machine inner diameter (mm)	30	30	30	30
Machine outer diameter (mm)	90	90	90	90
Axial length (mm)	25	25	25	25
Air gap length (mm)	0.5	0.5	0.5	0.5
Number of turns of armature coil/phase	80	80	80	80
Packing factor	0.5	0.5	0.5	0.5
Rotor pole pitch (degree)	45	36	25.7	22.5
PM angle (degree)	38.7	36	22.8	18.9
PM thickness (mm)	2.22	2.34	2.7	3
Slot area (mm^2)	48.8	48	52	52
Armature stator axial length (mm)	14.2	13.66	14	14.3
Tip thickness (mm)	1	0.75	0.5	0.5
Rotor axial length (mm)	4.9	5.17	5	4.85
I_{rms} (A)	14.4	14.3	14.8	15
PM volume (mm^3)	13270	16588	16691	17509

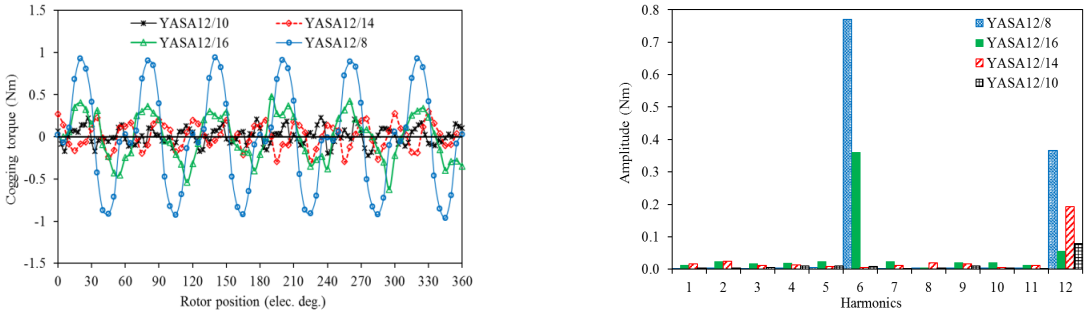

(a) Waveforms *(b) Harmonic spectra*

Figure 3: *Comparison of cogging torques of YASA machine topologies.*

3.2 No-Load Flux Density

The no-load flux density produced by the PM is one of the most essential for analyzing the PM machine performance. Figure 4 shows the flux distribution of the stator and rotor of YASA topologies. It can be seen that the topologies in which the rotor pole-arc is bigger than the stator pole-arc have a significant leakage flux since the effective magnet area is smaller than the full rotor pole-arc (i.e. YASA12/8), as indicated in Figure 4(a). Moreover, the saturation in the back iron is higher in YASA12/8 compared to the other topologies since the flux per pole is higher. Moreover, YASA12/14 has the highest flux density. In this case, the rotor pole-arc is approximately the same as the stator pole-arc without tips. Thus, the leakage flux is minimized, and the flux passed through the stator pole reaches its maximum value, as indicated in Figure 4(c). Furthermore, YASA12/16 has approximately the same flux density distribution as YASA12/14.

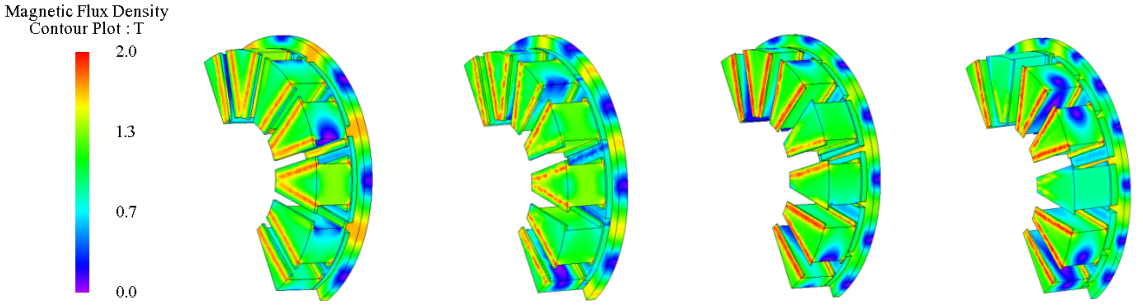

(a) YASA12/8 *(b) YASA12/10* *(c) YASA12/14* *(d) YASA12/16*

Figure 4: *Stator and rotor flux density distributions of YASA machine topologies.*

3.3 No-Load Flux Linkage and Back EMF

The no-load phase flux linkages of YASA machine topologies are analysed and compared in

Figure **5**. It is clear that YASA12/8 followed by YASA12/10 have the largest flux linkage amplitude while YASA12/16 has the smallest flux linkage amplitude. However, YASA12/8 flux harmonics include certain odd order harmonics, such as 3rd, 5th, and 7th, which make the flux linkage nonsinusoidal compared to the other topologies. Moreover, the no-load phase back EMFs of the YASA machines are studied and compared at a rotor speed of 400 rpm. Figure 6 shows the comparison of the back EMF and the corresponding harmonics for YASA topologies. YASA12/14 has the largest back EMF fundamental amplitude of approximately 4.26 V, whereas the EMF fundamental amplitude of YASA12/16 of approximately 4.25 V is just below YASA12/14. On the other hand, the amplitude of the fundamental harmonic of YASA12/10 is approximately 3.9 V, however, YASA12/8 has a non-sinusoidal waveform and contains odd order harmonics in which the amplitude of the fundamental component is approximately 3.3 V, as can be seen in Figure 6(b).

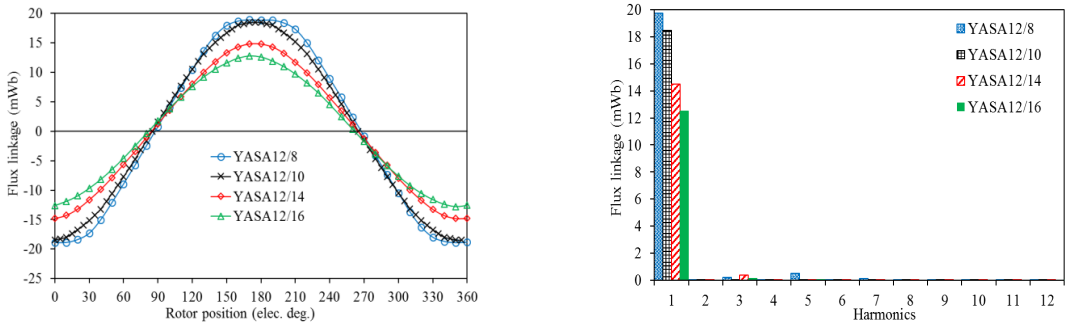

(a) Waveforms *(b) Harmonic spectra*

Figure 5: *Comparison of phase flux linkages of YASA machine topologies.*

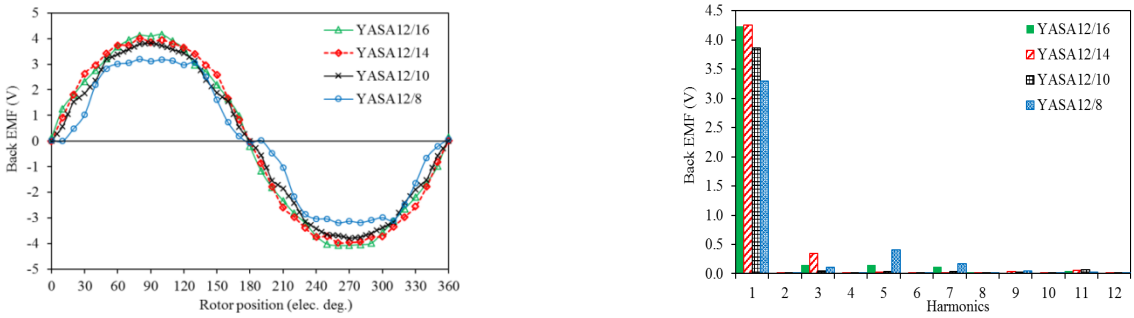

(a) Waveforms *(b)Harmonic spectra*

Figure 6: *Comparison of phase back EMFs of YASA machine topologies at 400 rpm.*

3.4 Electromagnetic Torque

The electromagnetic torque is studied and compared at rated current and the same machine speed. Figure 7 shows a comparison between YASA topologies in terms of the electromagnetic torque and the current angle relation at rated current, and Figure 8 compares the electromagnetic torque for YASA machines with different pole combinations. It is clear that, YASA12/16 and YASA12/14 have nearly the same highest torque while YASA12/8 has the lowest torque in which the leakage flux is high due to the magnet pitch being much bigger than the slot pole pitch. On the other hand, as can be seen in Figure 8(b), YASA12/14 has the lowest torque ripple followed by YASA12/10. YASA12/8 has the highest torque ripple compared to the other topologies.

Figure 9 shows a comparison between the proposed YASA machine topologies with respect to the torque, torque ripple and cogging torque. The cogging torque and torque ripple are calculated with reference to the average torque by:

$$T_{\text{ripple}}, T_{cog} = \frac{T_{\max} - T_{\min}}{T_{\text{avg}}} \times 100\ \% \qquad (5)$$

It should be noted that the preceding formula is used to calculate the cogging torque at no load and the torque ripple at load. The figure shows that YASA12/14 has a superior torque performance compared to the other topologies while YASA12/8 has high cogging torque and torque ripple.

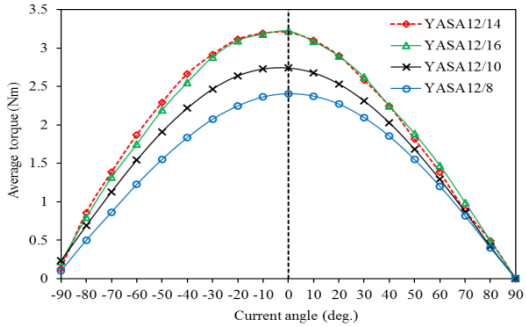

Figure 7: *Comparison of torque-current angle curves of YASA machine topologies.*

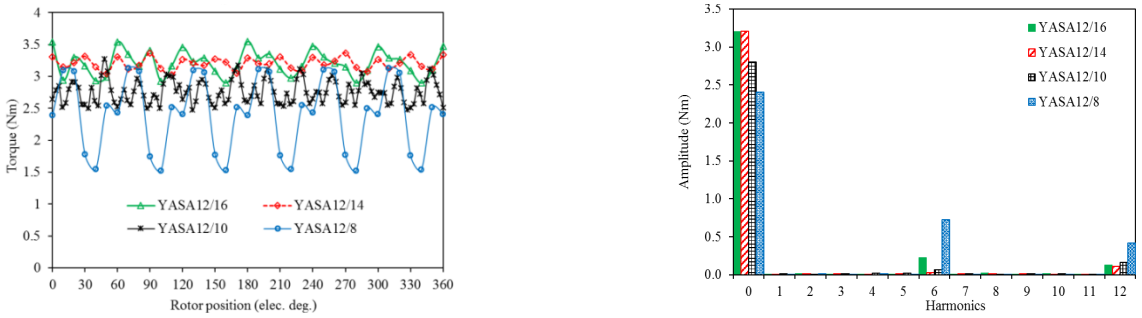

(a) Waveforms *(b) Harmonic spectra*

Figure 8: *Comparison of electromagnetic torques of YASA machine topologies.*

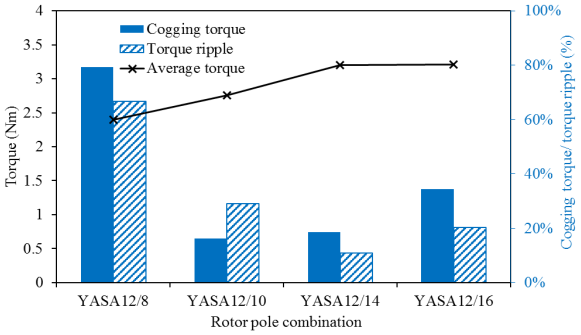

Figure 9: *Comparison of average torque, torque ripple and peak-peak cogging torque of YASA machine topologies*

4 Conclusion

In this paper, YASA machines with the same number of stator segments and different rotor pole number combinations with a high winding factor were chosen and designed with the aid of 3D-FEA. Moreover, a performance comparison between the YASA machine topologies with different rotor pole numbers has been verified. The results show that both YASA12/14 and YASA12/16 machines have higher no-load and on-load performances. Moreover, such topologies have higher back EMF and average torque; however, YASA12/16 has a noticeably higher cogging torque and torque ripple with the reference of YASA12/14. Furthermore, YASA12/8 has the smallest average torque and highest cogging torque and torque ripple compared to the other topologies. Overall, YASA12/14 and YASA12/16 both have a higher torque density in which both have approximately the same optimal magnet and stator active areas.

5 References

[1] T. J. Woolmer and M. D. McCulloch, "Axial flux permanent magnet machines: A new topology for high performance applications," in *IET - The Institution of Engineering and Technolgy Hybrid Vehicle Conference 2006*, 12-13 Dec. 2006, pp. 27-42.

[2] T. J. Woolmer and M. D. McCulloch, "Analysis of the Yokeless And Segmented Armature Machine," in *2007 IEEE International Electric Machines & Drives Conference*, 3-5 May 2007 2007, vol. 1, pp. 704-708.

[3] H. Vansompel, P. Sergeant, and L. Dupré, "Optimized Design Considering the Mass Influence of an Axial Flux Permanent-Magnet Synchronous Generator With Concentrated Pole Windings," *IEEE Transactions on Magnetics,* vol. 46, no. 12, pp. 4101-4107, 2010.

[4] F. G. Capponi, G. D. Donato, and F. Caricchi, "Recent Advances in Axial-Flux Permanent-Magnet Machine Technology," *IEEE Transactions on Industry Applications,* vol. 48, no. 6, pp. 2190-2205, 2012.

[5] W. Fei, P. C. K. Luk, and K. Jinupun, "A new axial flux permanent magnet Segmented-Armature-Torus machine for in-wheel direct drive applications," in *2008 IEEE Power Electronics Specialists Conference*, 15-19 June 2008 2008, pp. 2197-2202.

[6] S. T. Vun, M. D. McCulloch, and C. Y. Leong, "The development of an electromagnetic analytical design tool for megawatt-scale YASA generators," in *IET Conference on Renewable Power Generation (RPG 2011)*, 6-8 Sept. 2011 2011, pp. 1-6.

[7] N. J. Stannard, J. G. Washington, and G. J. Atkinson, "A comparison of axial field topologies employing SMC for traction applications," in *2016 19th International Conference on Electrical Machines and Systems (ICEMS)*, 13-16 Nov. 2016 2016, pp. 1-6.

[8] D. Ishak, Z. Q. Zhu, and D. Howe, "Permanent-magnet brushless machines with unequal tooth widths and similar slot and pole numbers," *IEEE Transactions on Industry Applications,* vol. 41, no. 2, pp. 584-590, 2005.

[9] J. Wang, K. Atallah, Z. Q. Zhu, and D. Howe, "Modular Three-Phase Permanent-Magnet Brushless Machines for In-Wheel Applications," *IEEE Transactions on Vehicular Technology,* vol. 57, no. 5, pp. 2714-2720, 2008.

[10] J. Cros and P. Viarouge, "Synthesis of high performance PM motors with concentrated windings," *IEEE Transactions on Energy Conversion,* vol. 17, no. 2, pp. 248-253, 2002.

[11] N. Bianchi and M. D. Pre, "Use of the star of slots in designing fractional-slot single-layer synchronous motors," *IEE Proceedings - Electric Power Applications,* vol. 153, no. 3, pp. 459-466, 2006.

[12] M. Aydin, Z. Q. Zhu, T. A. Lipo, and D. Howe, "Minimization of Cogging Torque in Axial-Flux Permanent-Magnet Machines: Design Concepts," *IEEE Transactions on Magnetics,* vol. 43, no. 9, pp. 3614-3622, 2007.

[13] B. Xia, J. Shen, P. C. Luk, and W. Fei, "Comparative Study of Air-Cored Axial-Flux Permanent-Magnet Machines With Different Stator Winding Configurations," *IEEE Transactions on Industrial Electronics,* vol. 62, no. 2, pp. 846-856, 2015.

[14] Z. Q. Zhu and D. Howe, "Influence of design parameters on cogging torque in permanent magnet machines," *IEEE Transactions on Energy Conversion,* vol. 15, no. 4, pp. 407-412, 2000.